Mechanisms of active control of sound radiation from an opening with boundary installed secondary sources

Shuping Wang,[1] Jiancheng Tao,[1,a)] Xiaojun Qiu,[2] and Jie Pan[3]
[1]*Key Laboratory of Modern Acoustics and Institute of Acoustics, Nanjing University, Nanjing 210093, China*
[2]*Centre for Audio, Acoustics and Vibration, Faculty of Engineering and Information Technology, University of Technology, Sydney, New South Wales 2007, Australia*
[3]*School of Mechanical and Chemical Engineering, The University of Western Australia, Perth, Western Australia 6009, Australia*

(Received 30 January 2018; revised 2 May 2018; accepted 9 May 2018; published online 6 June 2018)

Previous work has demonstrated that installing secondary sources at the edge of a cavity opening can reduce sound radiation through it, but the mechanisms are not clear, which is investigated in this paper by using the modal decomposition method. It is found that a double layer edge system achieves better performance than a single layer system because secondary sources at the edge of the same layer cannot excite some modes effectively and those at different heights compensate this. There exists an upper limit frequency for the systems with boundary installed secondary sources, which is mainly decided by the length of the short side of the opening. More secondary source layers at the edge will increase the upper limit frequency. © *2018 Acoustical Society of America*.
https://doi.org/10.1121/1.5040139

[JFL] Pages: 3345–3351

I. INTRODUCTION

Openings in walls of enclosures or buildings are often necessary for lighting, air circulation and access; however, they reduce the sound transmission loss of the walls. Passive noise control methods, such as applying porous materials, micro-perforated absorbers, and quarter-wave resonators, have been proposed to attenuate noise radiation through openings, but these methods require that the opening be sealed and/or filled with materials or structures to achieve sufficient noise reduction.[1–3] Active noise control (ANC) is an alternative option, especially in the low frequency range. De Salis *et al*. reviewed various noise control techniques for natural ventilation openings and suggested using ANC to supplement conventional passive attenuation in the low frequency region.[4]

According to Huygens's principle, every point at a wave front may be considered as the source of secondary wavelets with a speed equal to the speed of the waves, so the sound power radiation from a noise source can be reduced if secondary sources are distributed over the entire transmission path with their strengths opposite to the strengths of secondary wavelets.[5] Elliott *et al*. investigated the fundamental problem of active control of incident sound with an array of secondary sources both in free field and through apertures.[6] A clear cut-off frequency for noise control in free space is found, and its wavelength is equal to the separation between uniformly spaced secondary sources. It was also found that when the size of the aperture is compatible with the acoustic wavelength, only a few secondary sources are necessary for good control while more secondary sources are needed if the size of the window is larger than the wavelength.

Active control has been applied to reduce noise that propagates into buildings through open windows. Murao *et al*. proposed to apply active acoustic shielding (AAS) cells at an open window and introduced a new multiple channel adaptive algorithm to enlarge the AAS window size.[7] In 2016, a modified multichannel Fx-LMS algorithm was proposed to reduce computation complexity by summing the secondary paths from all the secondary loudspeakers to each error microphone.[8] To avoid the use of error microphones for the ease of implementation and maintenance, Lam *et al*. installed the ANC system at the opening of a small bedroom with a two-panel sliding window, and discussed the limitations of the system and potential solutions.[9] Carme *et al*. integrated a loudspeaker line in the window joinery and combined it with passive control, and the system was able to reduce the noise level up to 30 dB compared to a typical window ajar.[10]

For a sound source inside an open cavity with sound solely transmitted through the opening to the outside, global control of sound radiation can be achieved if sufficient secondary sources are implemented at the opening to minimize the sound pressure and its normal gradient at the opening. The broadband control performance of a planar virtual sound barrier (PVSB) system has been investigated and experimentally confirmed.[11] It was later found that when the PVSB system is stable and there is no constraint on the output strengths of secondary sources, an independent system can provide the same noise reduction as the fully coupled system.[12]

Although a PVSB system can reduce sound radiation through openings, secondary sources over the entire opening are not practical to implement in some applications because secondary sources located in the middle of the opening sometimes affect normal functionalities of openings. Preliminary

a)Electronic mail: jctao@nju.edu.cn

research has been carried out on a single-layered secondary source array at the edge of the opening (single layer edge system, SLES); however, it was found that global ANC is only effective within a very limited frequency band.[13]

Recently, we proposed a double-layered secondary source arrangement at the edge of a cavity opening (double layer edge system, DLES), which can effectively reduce sound power radiation through openings.[14] The system achieves better performance than a SLES with the same number of secondary sources. This paper further investigates (1) the mechanisms of active control with boundary installed secondary sources; (2) the difference between the SLES, DLES, PVSB, and N layer edge system (NLES) and the reason why the DLES performs better than the SLES; (3) the upper limit effective control frequency for the SLES, DLES, and PVSB systems.

II. THEORY

The double layer edge system is illustrated in Fig. 1, where the secondary sources are installed at two different heights along the edge of the opening. The secondary sources in the upper and lower layers have the same x-y coordinates, and a primary sound source is inside the open cavity. All the five walls of the cavity are assumed to be rigid, so sound outside the cavity is solely that transmitted through the opening.

The total sound power of the primary source and secondary sources with a control effort constraint is defined as the cost function, which is[15]

$$J = \frac{1}{2}\left\{\mathrm{Re}\left[q_{\mathrm{p}}^{\mathrm{H}} p_{\mathrm{p}}\right] + \mathrm{Re}\left[\boldsymbol{q}_{\mathrm{s}}^{\mathrm{H}} \boldsymbol{p}_{\mathrm{s}}\right]\right\} + \beta \boldsymbol{q}_{\mathrm{s}}^{\mathrm{H}} \boldsymbol{q}_{\mathrm{s}}, \tag{1}$$

where q_{p} is the strength of the primary source, p_{p} is the sound pressure at the position of the primary source, $\boldsymbol{q}_{\mathrm{s}}$ is the vector of the strengths of secondary sources, and $\boldsymbol{p}_{\mathrm{s}}$ is the vector of the sound pressure at the positions of secondary sources. β is a real number to constrain the outputs of secondary sources.[15,16] After minimizing Eq. (1), the optimized strengths of secondary sources can be obtained with

$$\boldsymbol{q}_{\mathrm{s}} = -(\boldsymbol{R}_{\mathrm{ss}} + \beta \mathbf{I})^{-1} \boldsymbol{R}_{\mathrm{sp}} q_{\mathrm{p}}, \tag{2}$$

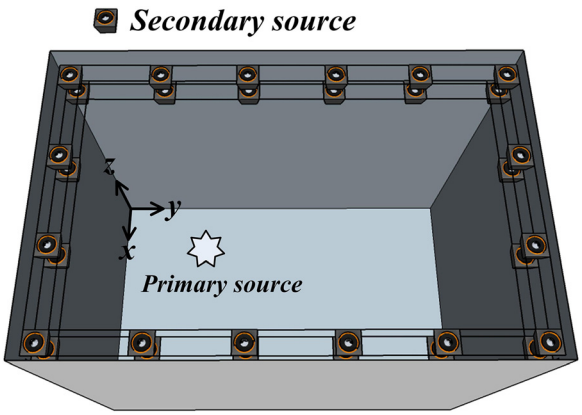

FIG. 1. (Color online) Schematic diagram of a DLES.

where $\boldsymbol{R}_{\mathrm{ss}}$ and $\boldsymbol{R}_{\mathrm{sp}}$ are the real parts of $\boldsymbol{Z}_{\mathrm{ss}}$ and $\boldsymbol{Z}_{\mathrm{sp}}$. $\boldsymbol{Z}_{\mathrm{ss}}$ is the acoustic transfer function matrix between the secondary sources, $\boldsymbol{Z}_{\mathrm{sp}}$ is the acoustic transfer function vector between the primary source and secondary sources, and $\mathbf{I}$ is an identity matrix. The noise reduction is defined as the difference between the sound power level without and with control

$$\mathrm{NR} = 10 \log_{10} \frac{W_{\mathrm{off}}}{W_{\mathrm{on}}}, \tag{3}$$

where W_{off} is the total sound power without active control and W_{on} is that with control. W_{off} can be calculated as the integral of sound intensity over the opening area S,

$$W_{\mathrm{off}} = \int\int_S \frac{1}{2}\mathrm{Re}\left\{p_{\mathrm{po}}(x,y)^* v_{\mathrm{po}}(x,y)\right\} \mathrm{d}x\,\mathrm{d}y, \tag{4}$$

in which $p_{\mathrm{po}}(x,y)$ is the primary sound pressure and $v_{\mathrm{po}}(x,y)$ is the primary normal particle velocity at (x,y,l_y) at the opening. p_{po} and v_{po} can be expressed as a superposition of a series of modes of an infinitely long rectangular rigid duct $\phi_m(x,y)$,[17]

$$p_{\mathrm{po}}(x,y) = \sum_{m=1}^{L} P_{\mathrm{p}m}\phi_m(x,y), \tag{5}$$

$$v_{\mathrm{po}}(x,y) = \sum_{m=1}^{L} V_{\mathrm{p}m}\phi_m(x,y), \tag{6}$$

$$\phi_m(x,y) = \cos\frac{m_x\pi}{l_x}x \cos\frac{m_y\pi}{l_y}y, \tag{7}$$

where $P_{\mathrm{p}m}$ and $V_{\mathrm{p}m}$ are the modal amplitudes of the sound pressure and particle velocity, respectively, of the mth mode excited by the primary source. The dimension of the cavity is $l_x \times l_y \times l_z$.

Because of the orthogonality of $\phi_m(x,y)$, the contribution of the mth mode to the total sound power is

$$W_{\mathrm{off}\_m} = \frac{1}{2}\mathrm{Re}\left[q_{\mathrm{p}}^* P_{\mathrm{p}m}{}^* \Lambda_m V_{\mathrm{p}m} q_{\mathrm{p}}\right], \tag{8}$$

where

$$\Lambda_m = \int\int_S \phi_m(x,y)\phi_m(x,y)\,dx\,dy = \begin{cases} S, & m_x = m_y = 0 \\ \frac{S}{2}, & m_x = 0, m_y \neq 0, \text{or } m_x \neq 0, m_y = 0 \\ \frac{S}{4}, & m_x \neq 0, m_y \neq 0. \end{cases} \tag{9}$$

With active control, the sound pressure and normal particle velocity at the opening are the contributions of both the primary source and all the N secondary sources, thus, the total sound power is

$$W_{\mathrm{on}} = \int\int_S \frac{1}{2}\mathrm{Re}\left\{[p_{\mathrm{po}} + p_{\mathrm{so}}]^*[v_{\mathrm{po}} + v_{\mathrm{so}}]\right\} dS, \tag{10}$$

where p_{so} and v_{so} are the sums of the contributions of N secondary sources

$$p_{so} = \sum_{i=1}^{N}\sum_{m=1}^{L} P_{im}\phi_m(x,y), \tag{11}$$

$$v_{so} = \sum_{i=1}^{N}\sum_{m=1}^{L} V_{im}\phi_m(x,y), \tag{12}$$

and P_{im} and V_{im} are the modal amplitudes of sound pressure and particle velocity, respectively, of the mth mode excited by the ith secondary source.

The contribution of the mth mode to the total sound power with control can be calculated by combining Eqs. (10)–(12),

$$W_{on\_m} = \frac{1}{2}\mathrm{Re}\left[q_p{}^* P_{pm}{}^* \Lambda_m V_{pm} q_p + q_p{}^* P_{pm}{}^* \Lambda_m \sum_{i=1}^{N} q_i V_{im} + q_p V_{pm} \Lambda_m \sum_{i=1}^{N} q_i{}^* P_{im}{}^* + \sum_{i=1}^{N}\sum_{j=1}^{N} q_i{}^* P_{im}{}^* \Lambda_m V_{jm} q_j\right], \tag{13}$$

where q_i and q_j are the optimized strengths of the ith and jth secondary sources, respectively. The total sound power can be calculated by the sum of all the modal sound powers.

According to Ref. 11, the sound pressure excited at the opening by the ith secondary source with the strength q_i can be expressed as

$$p_i(x,y) = \sum_{m=1}^{N}\left(P_m^{\mathrm{i}} e^{-jk_{mz}l_z} + P_m^{\mathrm{r}} e^{jk_{mz}l_z}\right)\phi_m(x,y) + \frac{\rho_0 \omega q_i}{2S}\sum_{m=1}^{N}\frac{\phi_m(x_i,y_i)\phi_m(x,y)}{\Lambda_m k_{mz}} \times \exp(-jk_{mz}|l_z - z_i|), \tag{14}$$

where P_m^{i} and P_m^{r} are two coefficients that can be obtained with the boundary conditions at the bottom and opening of the cavity. ρ_0 is the density of the air and ω is the angular frequency. The mth modal amplitude of sound pressure excited by the ith secondary source is

$$P_{im} = P_m^{\mathrm{i}} e^{-jk_{mz}l_z} + P_m^{\mathrm{r}} e^{jk_{mz}l_z} + \frac{\rho_0 \omega q_i \phi_m(x_i,y_i)}{2S\Lambda_m k_{mz}} \times \exp(-jk_{mz}|l_z - z_i|), \tag{15}$$

and the mth modal particle velocity can be calculated with

$$V_{im} = \frac{1}{j\rho_0\omega}\frac{\partial P_{im}}{\partial z}. \tag{16}$$

III. RESULTS AND DISCUSSIONS

A. Mechanism study

In the simulations, the dimension of the open cavity is 0.4 m × 1.0 m × 1.5 m ($l_x \times l_y \times l_z$), and the size of the opening is 0.4 m × 1.0 m. Because it is complicated to calculate the sound field in the case of an unbaffled open cavity,[18,19] the opening is assumed to be embedded at an infinite rigid baffle, and the modal superposition method in Ref. 11 is applied to obtain the theoretical acoustic transfer functions and the sound pressure at the opening. The modal terms included in the simulations [N in Eq. (14)] are chosen according to the frequency to guarantee the convergence of calculation. For example, N is chosen as 80 for 1100 Hz and 120 for 2280 Hz. The optimized strengths of secondary sources are obtained by Eq. (2).

Thirty-two secondary sources are used in the DLES, SLES, and PVSB systems. Figure 2 shows the plan view of the specific positions of the secondary sources in the three configurations in the x-y plane. In the DLES, two sets of 16 secondary sources are distributed at the edge of the $z = 1.4$ m (Nos. 1–16) and $z = 1.45$ m planes (Nos. 17–32), respectively, and the two sets are at the same positions in the x-y plane. Secondary sources Nos. 1–16 in the SLES and PVSB are at the same positions as those in the DLES. Secondary

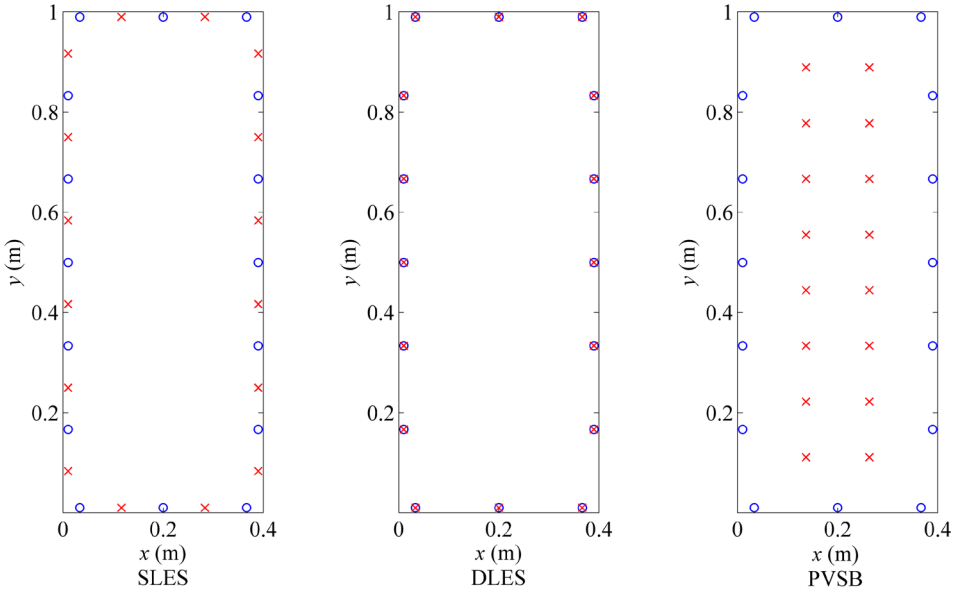

FIG. 2. (Color online) The plan view of the positions of 32 secondary sources in the x-y plane in the SLES, DLES, and PVSB, where "○" corresponds to secondary sources Nos. 1–16, which are the same for the three systems, and "×" corresponds to secondary sources Nos. 17–32.

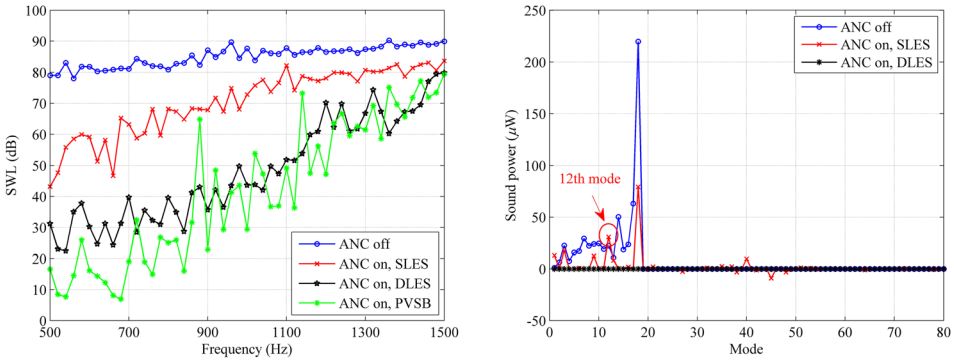

FIG. 3. (Color online) The sound power level (SWL) and modal sound power with and without ANC, (a) SWL, (b) the modal sound power at 1100 Hz.

sources Nos. 17–32 are also at the edge of the $z = 1.4$ m plane in the SLES, and in the PVSB system, they are evenly distributed in the middle of the $z = 1.4$ m plane. The primary source is set at (0.01,0.01,0.01) m.

Figure 3(a) shows the sound power level without and with control under the three configurations. The DLES achieves much better performance than the SLES, especially at high frequencies. Take 1100 Hz as an example, the sound power reduction at 1100 Hz is 5.6 dB and 37.1 dB with the SLES and DLES, respectively. The modal decomposition method is applied to explain the reason why the DLES outperforms. The modes are sorted according to their modal frequencies and the first 20 modes and their corresponding modal frequencies are listed in Table I. Figure 3(b) shows the modal sound power W_m of the first 80 modes at 1100 Hz without and with control. It can be observed that the total sound power of the primary sound field at 1100 Hz mainly concentrates in the first 18 modes, and this is evidence that including 80 modes in the calculation is sufficient. Each of the first 18 modal sound powers is almost completely suppressed after control with the DLES, while for the SLES, the 1st, 3rd, 9th, 12th, and 18th modal sound powers are not effectively attenuated, resulting in the lower reduction in sound power.

TABLE I. The first 20 mode numbers and the corresponding modal frequencies.

m	m_x	m_y	Frequency (Hz)
1	0	0	0.00
2	0	1	255.97
3	1	0	396.99
4	1	1	472.36
5	0	2	511.94
6	1	2	647.83
7	0	3	767.91
8	2	0	793.98
9	2	1	834.22
10	1	3	864.46
11	2	2	944.72
12	0	4	1023.88
13	1	4	1098.15
14	2	3	1104.58
15	3	0	1190.97
16	3	1	1218.17
17	0	5	1279.85
18	2	4	1295.66
19	3	2	1296.34
20	1	5	1340.01

Figure 4(a) shows the modal amplitudes of the sound pressure p and normal particle velocity v of the 12th mode excited by all the 32 secondary sources at 1100 Hz, which are obtained with Eqs. (15) and (16). It can be seen that the modal amplitudes corresponding to the 17th–32nd secondary sources in the DLES are much larger than those of the 1st–16th secondary sources. This indicates that secondary sources at the edge of the $z = 1.4$ m plane cannot excite the 12th mode effectively. Introducing secondary sources at a different height (e.g., $z = 1.45$ m) increases the noise reduction of the 12th mode and contributes to the reduction of the total sound power. Due to the limited modal amplitudes excited by the secondary sources in the SLES, the strengths of the secondary sources have to be sufficiently large to effectively suppress the mode, as shown in Fig. 4(b). This may result in control spillover,[20] as evidenced by the increase of, for example, the 40th mode as shown in Fig. 3(b).

Although secondary sources are at the same height as well in the PVSB system, they achieve much higher noise reduction than the SLES, as shown in Fig. 3(a). The sound power reduction at 1100 Hz is 38.6 dB with the PVSB. Figure 5 shows the modal amplitudes of p and v of the 40th mode excited by the 32 secondary sources in the SLES and PVSB system at 1100 Hz. The modal amplitudes corresponding to the 17th–32nd secondary sources in the PVSB system are much smaller than those of the rest of the secondary sources. This indicates that secondary sources in the middle of the opening are closer to the nodal lines of the 40th mode than those at the edge, thus, it avoids the control spillover and leads to higher noise reduction.

The DLES achieves much higher noise reduction than the SLES, but increasing the number of secondary sources at the edge of two layers does not infinitely improve the performance. As shown in Fig. 6(a), the sound power reductions corresponding to 88 and 172 secondary sources in the DLES are almost the same, which means that the performance will not be improved any more once the number reaches 88. However, it can be seen from Fig. 6(a) that if 44 secondary sources are added at the edge of another height $z = 1.35$ m at the same x-y positions as those in the DLES with 88

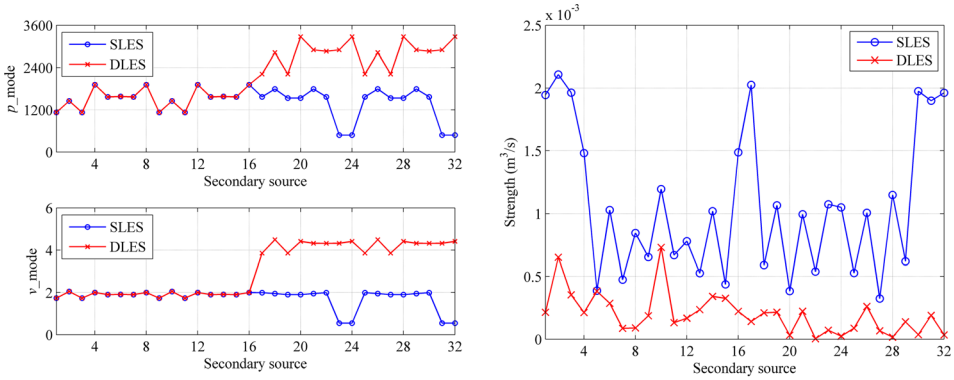

(a) (b)

FIG. 4. (Color online) The modal amplitudes and optimized strengths of secondary sources, (a) the amplitudes of p and v of the 12th mode excited by the 32 secondary sources in the SLES and DLES at 1100 Hz, (b) the optimized strengths of secondary sources in the SLES and DLES at 1100 Hz.

secondary sources, the 3 layer edge system (3LES) with 132 secondary sources significantly improves the noise reduction performance. Take 2280 Hz as an example, the sound power reduction is 10.4 dB with the DLES and 33.9 dB with the 3LES.

Figure 6(b) shows the first 120 modal sound powers at 2280 Hz. The total sound power of the primary sound field at 2280 Hz mainly concentrates in the first 70 modes, and this is evidence that including 120 modes in the calculation is sufficient. It can be seen from Fig. 6(b) that the DLES cannot suppress all the modes effectively, for example, the 55th mode. The amplitudes of p and v of the 55th mode excited by the 88 secondary sources in the DLES and 132 secondary sources in the 3LES are shown in Fig. 6(c). It is obvious that the secondary sources in the 3rd layer (Nos. 89–132) excite the 55th mode more effectively because they are at a different height from the other 2 layers. This is the reason that the 3LES performs better than the DLES. Because the modes can be excited more effectively, the optimized strengths of secondary sources in the 3LES are much smaller than those of the secondary sources in the DLES, as shown in Fig. 6(d). There are certain modes that secondary sources at the same layer cannot effectively excite, and introducing those at other layers can compensate it, which helps improve the noise reduction performance. It can be expected that an NLES with $N > 3$ will further improve the performance.

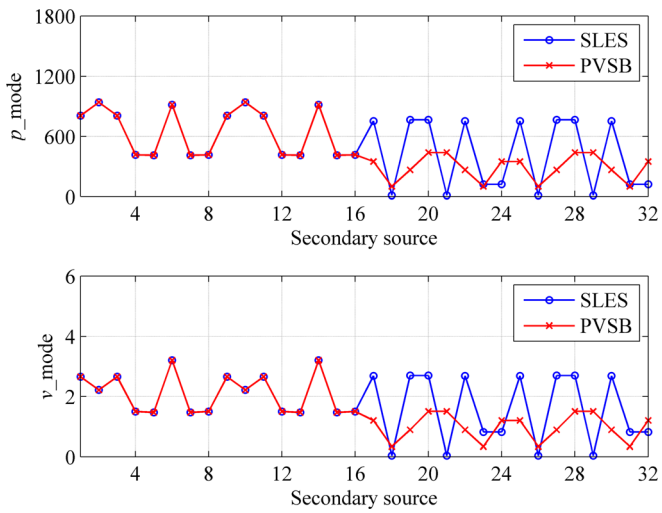

FIG. 5. (Color online) The amplitudes of p and v of the 40th mode excited by the 32 secondary sources in the SLES and PVSB system at 1100 Hz.

B. Upper limit frequency for effective control

Section III A shows that increasing the number of secondary sources in the DLES cannot infinitely improve the control performance. Using 20 dB as the threshold, the highest frequency at which the sound power reduction is more than 20 dB is defined as f_{20}. Figure 7 shows the half wavelength of f_{20} as a function of the interval between secondary sources in the PVSB, SLES, DLES, and 3LES. In the PVSB system, the secondary sources are evenly distributed at the $z = 1.4$ m plane with the same intervals along both the x and y axes. In the SLES, DLES, and 3LES, the secondary sources are evenly distributed along the boundaries. It can be seen that f_{20} of the PVSB system increases when the interval between secondary sources becomes smaller and sound radiation at any frequency can be reduced as long as there are a sufficient number of secondary sources. The black line is the fitted curve for the PVSB and the half wavelength of f_{20} is close to the interval between secondary sources, especially when the interval between secondary sources is small.

Another observation from Fig. 7 is that unlike the PVSB system, f_{20} for the system with boundary installed secondary sources increases when the interval between secondary sources becomes smaller at first, but once the interval reduces to a certain value, it remains the same. This frequency is defined as the upper limit frequency, which is the highest frequency at which the sound radiation can be effectively reduced with sufficiently many secondary sources. Finally, more secondary source layers increase f_{20} with the same interval between secondary sources.

Figure 8(a) shows the upper limit frequency of the SLES, DLES, and 3LES as a function of l_x when l_y is fixed as 1.0 m and $l_z = 1.5$ m. There are sufficient secondary sources at the edge to achieve the best noise reduction performance. It can be seen that more layers increase the upper limit frequency and when l_x is much smaller than l_y, the upper limit frequency increases significantly. It can also be found that the upper limit frequency depends mainly on the short side of the opening because it changes very little after l_x increases to 1.0 m. This is further demonstrated by the results for a flat opening (l_x is much smaller than l_y) shown in Fig. 8(b), where the wavelengths corresponding to the

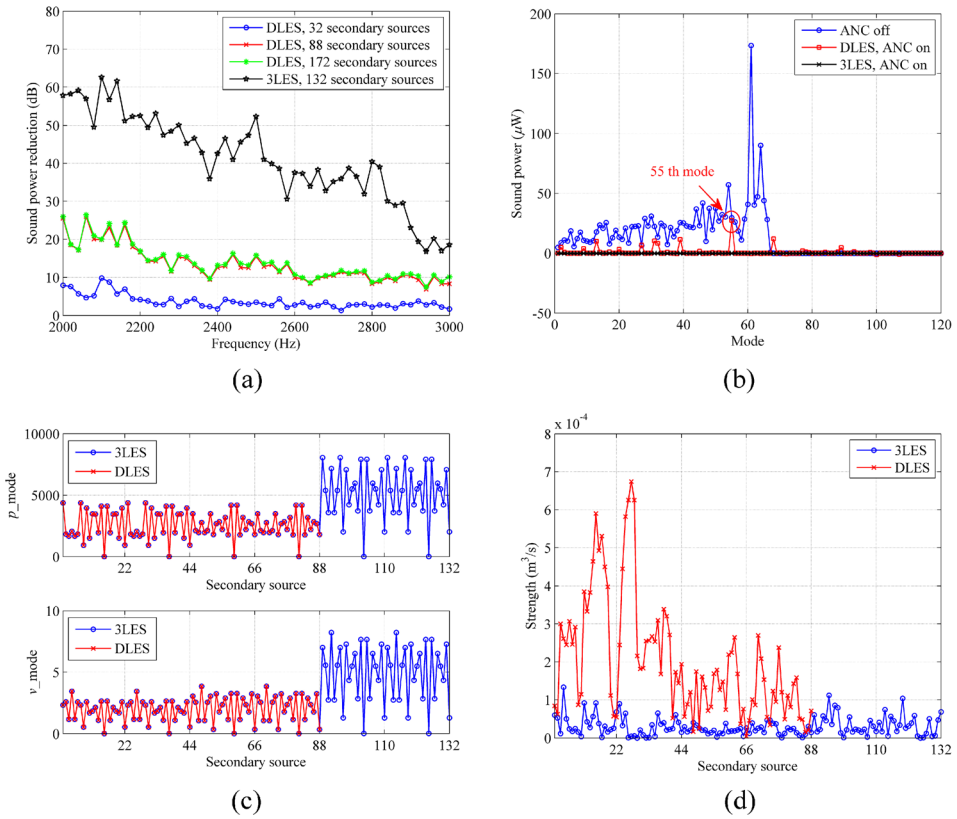

FIG. 6. (Color online) Performance analysis of the DLES and 3 layer edge system (3LES) systems, (a) the sound power reduction, (b) the first 120 modal sound powers at 2280 Hz without and with ANC, (c) the amplitudes of p and v of the 55th mode excited by the 88 secondary sources in the DLES and 132 secondary sources in the 3LES at 2280 Hz, (d) the optimized strengths of the secondary sources in the DLES and 3LES at 2280 Hz.

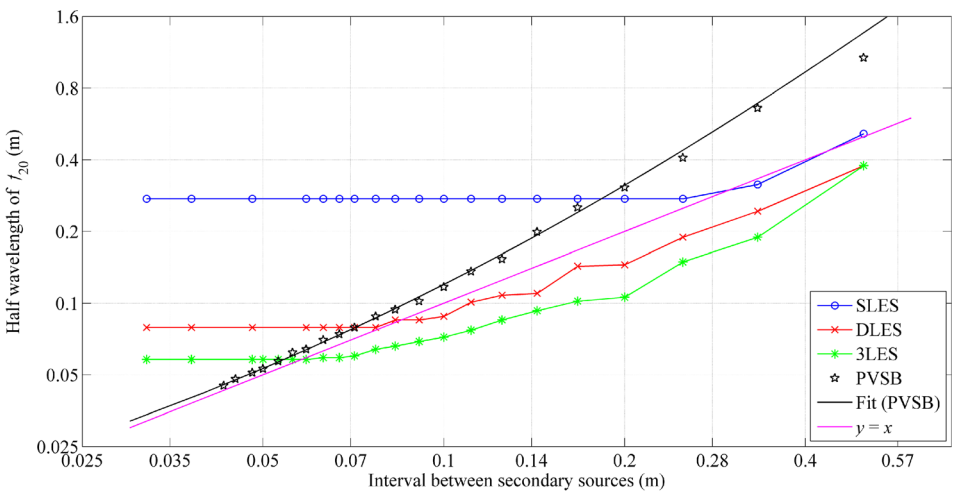

FIG. 7. (Color online) The half wavelength of f_{20} as a function of the interval between secondary sources in the PVSB, SLES, DLES, and 3LES.

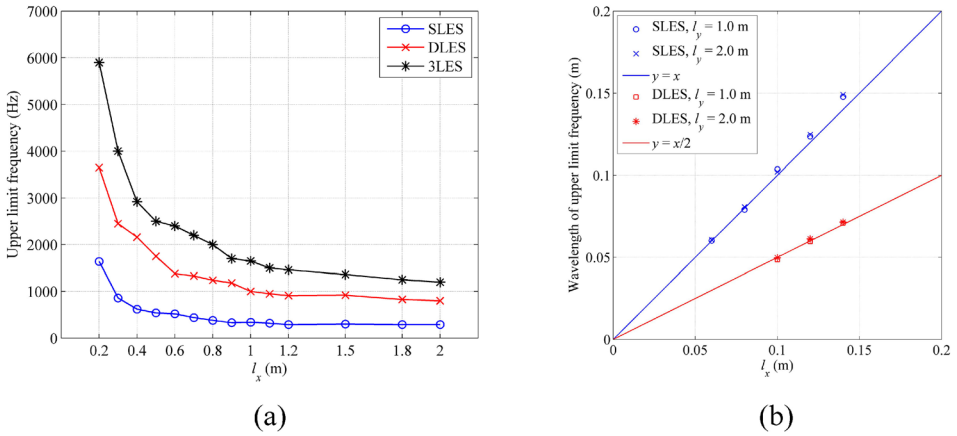

FIG. 8. (Color online) The upper limit frequency of the SLES, DLES, and 3LES systems, (a) the upper limit frequency of the SLES, DLES, and 3LES as a function of l_x when $l_y = 1.0$ m and $l_z = 1.5$ m, (b) the wavelength of the upper limit frequency as a function of l_x when $l_y = 1.0$ m and 2.0 m, $l_z = 1.5$ m.

upper limit frequency of the SLES and DLES are approximately l_x and $l_x/2$, respectively, and remain the same when l_y is different.

IV. CONCLUSIONS

The modal decomposition method is used to explain why the DLES achieves better noise reduction performance than the SLES. The reason is that secondary sources at the edge of the same layer cannot excite some modes effectively while those at the other height in the DLES compensate it. Secondary sources in the middle of the opening in the PVSB system are closer to the nodal lines of some modes than those at the edge, which lower the possibility of control spillover and result in higher noise reduction. It is also found that there exists an upper limit frequency for the SLES, DLES, and 3LES and more secondary source layers increase the upper limit frequency. The upper limit frequency mainly depends on the length of the short side of the opening, especially for a flat opening.

ACKNOWLEDGMENTS

This research was supported by the National Science Foundation of China (Grant No. 11474163) and under the Australian Research Council's Linkage Projects funding scheme (Grant No. LP140100987).

[1]F. Asdrubali and F. Cotana, "Influence of filtering system on high sound insulation ventilating windows," in *Proceedings of Inter-Noise* (1999).
[2]J. Kang and M. W. Brocklesby, "Feasibility of applying micro-perforated absorbers in acoustic window systems," Appl. Acoust. **66**, 669–689 (2005).
[3]C. D. Field and F. R. Fricke, "Theory and applications of quarter-wave resonators: A prelude to their use for attenuating noise entering buildings through openings," Appl. Acoust. **53**, 117–132 (1998).
[4]M. De Salis, D. Oldham, and S. Sharples, "Noise control strategies for naturally ventilated buildings," Build. Environ. **37**(5), 471–484 (2002).
[5]P. Nelson and S. Elliott, *Active Control of Sound* (Academic, London, 1992).
[6]S. Elliott, J. Cheer, B. Lam, C. Shi, and W. Gan, "Controlling incident sound fields with source arrays in free space and through apertures," in *Proceedings of the 24th International Congress on Sound and Vibration*, London (2017).
[7]T. Murao, M. Mishimura, L. Sakurama, and S. Nishida, "Basic study on active acoustic shielding: Phase 6 improving the method to enlarge AAS window-2," in *Proceedings of Inter-Noise*, Melbourne (2014).
[8]T. Murao, M. Nishimura, J. He, B. Lam, R. Ranjan, C. Shi, and W. Gan, "Feasibility study on decentralized control system for active acoustic shielding," in *Proceedings of Inter-Noise*, Hamburg (2016).
[9]B. Lam, C. Shi, and W. Gan, "Active noise control systems for open windows: Current updates and future perspectives," in *Proceedings of the 24th International Congress on Sound and Vibration*, London (2017).
[10]C. Carme, O. Schevin, C. Romerowski, and J. Clavard, "Active opening windows," in *Proceedings of the 23rd International Congress on Sound and Vibration*, Athens (2016).
[11]S. Wang, J. Tao, and X. Qiu, "Performance of a planar virtual sound barrier at the baffled opening of a rectangular cavity," J. Acoust. Soc. Am. **138**(5), 2836–2847 (2015).
[12]J. Tao, S. Wang, X. Qiu, and J. Pan, "Performance of an independent planar virtual sound barrier at the opening of a rectangular enclosure," Appl. Acoust. **105**, 215–223 (2016).
[13]S. Wang, J. Yu, X. Qiu, M. Pawelczyk, A. Shaid, and L. Wang, "Active sound radiation control with secondary sources at the edge of the opening," Appl. Acoust. **117**, 173–179 (2017).
[14]S. Wang, J. Tao, and X. Qiu, "Controlling sound radiation through an opening with secondary loudspeakers along its boundaries," Sci. Rep. **7**, 13385 (2017).
[15]S. Elliott, P. Joseph, P. Nelson, and M. Johnson, "Power output minimization and power absorption in the active control of sound," J. Acoust. Soc. Am. **90**(5), 2501–2512 (1991).
[16]O. Kirkeby, P. Nelson, F. Orduna-Bustamante, and H. Hamada, "Local sound field reproduction using digital signal processing," J. Acoust. Soc. Am. **100**(3), 1584–1593 (1996).
[17]P. Morse and K. Ingard, *Theoretical Acoustics* (MacMillan, London, 1986), p. 504.
[18]G. F. Homicz and J. A. Lordi, "A note on the radiative directivity patterns of duct acoustic modes," J. Sound Vib. **41**(3), 283–290 (1975).
[19]H. Levine and J. Schwinger, "On the radiation of sound from an unflanged circular pipe," Phys. Rev. **73**(4), 383–406 (1948).
[20]L. Gaudiller and J. D. Hagopian, "Active control of flexible structures using a minimum number of components," J. Sound Vib. **193**(3), 713–741 (1996).